Lecture Notes by Jürgen Vollmer

Theoretical Mechanics

— Working Copy — Chapter 6 —

— 2021-10-07 04:51:19+02:00—

Fakultät für Physik und Geowissenschaften, Universität Leipzig

LECTURES DELIVERED AT FAKULTÄT FÜR PHYSIK UND GEOWISSENSCHAFTEN, UNIVERSITÄT LEIPZIG
http://www.uni-leipzig.de/physik/~vollmer

Contents

6
Integrable Dynamics

In Chapter 5 we considered objects that consist of a mass points with fixed relative positions, like a flying and spinning ping-pong ball. Rather than providing a description of each individual mass element, we established equations of motion for their center of mass and the orientation of the body in space. From the perspective of theoretical mechanics the fixing of relative positions is a constraint to their motion, just as the ropes of a swing enforces a motion on a one-dimensional circular track, rather than in two dimensions. The deflection angle θ of the pendulum, and the center of mass and orientation of the ball are examples of generalized coordinates that automatically take into account the constraints.

In this chapter we discuss how to set up generalized coordinates and how to find the associated equations of motion. The discussion will be driven by examples. The examples will be derived from the realm of integrable dynamics. These are systems where conservation laws can be used to break down the dynamics into separate problems that can be interpreted as motion with a single degree of freedom.

At the end of the chapter you know why coins run away rolling on their edge, and how the speed of a steam engine was controlled by a mechanical device. Systems where the dynamics is not integrable will subsequently be addressed in Chapter 7.

add more pics

Marguerite Martyn, 1914
wikimedia/public domain

Figure 6.1: The point-particle idealization of a girl on a swing is the mathematical pendulum of Figures 1.2 and 1.3.

6.1 Motivation and Outline: How to deal with constraint motion?

Almost all interesting problems in mechanics involve constraints due to rails or tracks, and due to mechanical joints of particles. The most elementary example is a swing (Figure 6.1), where a rope forces a mass M to move on a path with positions constrained to a circle with radius given by the length L of the rope. Gravity $M\,\boldsymbol{g}$ and the pulling force $\boldsymbol{F}_r$ of the rope acting act on the mass (Figure 6.2). However, how large is the latter force? At the topmost point of its trajectory the mass is at rest, and no force is needed along the rope to keep it on its track. At the lowermost point, where the swing goes with its maximum speed, there is a substantial force. Newton's formalism requires a discussion of these forces. Lagrange established an alternative approach that provides equations of motion with substantially less effort. The key idea of this formalism is to select generalized coordinates adapted to the problem.

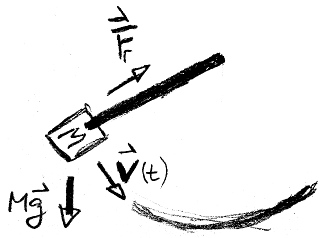

Figure 6.2: Forces acting for the motion of a swing, or its equivalent idealization of of a mathematical pendulum.

Definition 6.1: Generalized Coordinates

We consider N particles moving in D dimensions. Their motion is constrained to lie on a prescribed track and their relative positions may be constrained by bars and joints. Due to the constrains the system only has $M < D\,N$ degrees of freedom. In this chapter we denote the positions of the particles as $\boldsymbol{x} \in \mathbb{R}^{D\,N}$, and we specify position compatible with the constraints as $\boldsymbol{x}(\boldsymbol{q}(t))$, where $\boldsymbol{q} \in \mathbb{R}^{M}$ are the *generalized coordinates* adapted to the constrained motion.

Example 6.1: Generalized coordinates for a pendulum

We describe the position of the mass in a mathematical pendulum by the angle $\theta(t)$, as introduced in Example 1.10. The position of the mass in the 2D pendulum plane is thus described by the vector

$$\boldsymbol{x}(t) = L \begin{pmatrix} \sin\theta(t) \\ -\cos\theta(t) \end{pmatrix} = L\,\hat{\boldsymbol{R}}(\theta(t))\,.$$

In view of the chain rule its velocity amounts to

$$\dot{\boldsymbol{x}} = L\,\dot\theta\,\partial_\theta \hat{\boldsymbol{R}}(\theta(t)) = L\,\dot\theta\,\hat{\boldsymbol{\theta}}(\theta(t)) \quad \text{with} \quad \hat{\boldsymbol{\theta}}(\theta(t)) = \begin{pmatrix} \cos\theta(t) \\ \sin\theta(t) \end{pmatrix}$$

Note that $\hat{\boldsymbol{R}}(\theta)$ and $\hat{\boldsymbol{\theta}}(\theta)$ are orthonormal vectors that describe the position of the mass in terms of polar coordinates rather than fixed-in-space Cartesian coordinates.

Example 6.2: Generalized coordinates for a ping-pong ball

A ping-pong ball consists of N atoms located in the three-dimensional space. During a match they follow an intricate trail in the vicinity of the ping-pong players. At any time during their motion the atoms are located on a thin spherical shell with fixed positions with respect to each other. Rather than specifying the position of each atom one can therefore specify the position of the ball in terms of six generalized coordinates (Figure 6.3): Three coordinates provide its center of mass. The orientation of the ball can be provided by specifying the orientation of a body fixed axis in terms of its polar and azimuthal angle, and a third angle specifies the orientation of a point on its equator when rotating the ball around the axis.

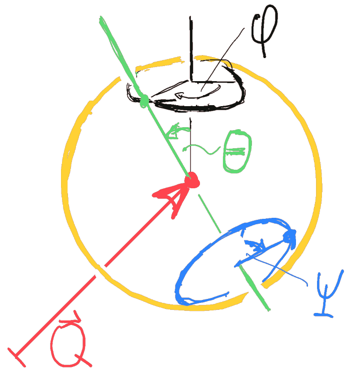

Figure 6.3: The position of a ball in space can be described in terms of a 3D vector $\boldsymbol{Q}$ that describes the center of the ball (red dot), angles θ, ϕ that describe the orientation in space of a fixed axes in the ball (green line), and another angle ψ that describes the position of point that is not on the axis (blue point).

Generalized coordinates describe only positions complying with the constraints of the motion, and they do not account for other positions from the very beginning. Lagrange's key observation is that constraint forces, e. g. the force on the rope of the swing, only act in a direction orthogonal to the positions described by generalized coordinates. Therefore, the constraint forces do not affect the time evolution of generalized coordinates. For the pendulum and the ping-pong ball one only has to account for gravity to find the evolution of the generalized coordinates. There is no need to deal with the force along the rope in the swing, and the atomic interaction forces that keep atoms in their positions in the ping-pong ball.

Outline

In Section 6.2 we will introduce the Lagrange formalism that will allow us without much ado to determine the EOM for generalized coordinates. Subsequently, in Section 6.3 we deal with systems with a single degree of freedom. In Section 6.4 we will see how symmetries in the dynamics allow us to eliminate a second degree of freedom based on an informed choice of generalized coordinates. Section 6.5 deals with two-particle systems and other problems where one deals with several degrees of freedom. In all cases we will eventually reduce the dynamics to one-dimensional problems. The final Section 6.6 deals with the relation between continuous symmetries of the dynamics and conservation laws.

6.2 *Lagrange formalism*

The Lagrange formalism provides an effective approach to derive the EOM for generalized coordinates. We first provide a derivation in a Cartesian coordinate frame. Then we discuss how the EOM for generalized coordinates are determined.

6.2.1 *Euler-Lagrange equations for Cartesian coordinates*

In Section 5.5 we saw that at mobile will be at rest in a position characterized by the coordinate vector $\boldsymbol{x}$ when the leading order correction $\delta\boldsymbol{x} \cdot \nabla\Phi(\boldsymbol{x})$ to its potential energy $\Phi(\boldsymbol{x})$ vanishes for every perturbation $\delta\boldsymbol{x}$ of the position. In the following we denote the leading order corrections term of the Taylor expansion as variation.

Definition 6.2: Variation of a scalar function

Let $f : \mathbb{D} \times [t_I, t_E] \to \mathbb{R}$ with $\mathbb{D} \subset R^D$ be function that has continuous first derivatives for all $\boldsymbol{x} \in \mathbb{D}$. The *variation of* f for a small deviation $\delta\boldsymbol{x}$ of $\boldsymbol{x}$ such that $\boldsymbol{x} + \delta\boldsymbol{x} \in \mathbb{D}$ amounts to the linear-order term of the Taylor expansion of f,

$$\delta f(\boldsymbol{x}, t) = \delta\boldsymbol{x} \cdot \nabla_{\boldsymbol{x}} f(\boldsymbol{x}, t) = \sum_{i=1}^{D} \delta x_i \, \frac{\partial f(\boldsymbol{x}, t)}{\partial x_i}$$

In Section 5.5 we showed that $\delta\Phi(\boldsymbol{x}_0) = 0$ for every critical point $\boldsymbol{x}_0$ where the system is (and remains) at rest. We now also account fort explicitly time-dependent potentials $\Phi(\boldsymbol{x}, t)$ and consider the variations $\delta\boldsymbol{x}(t)$ of time dependent trajectories $\boldsymbol{x}(t)$ with $t \in [t_I, t_F]$. Here $\delta\boldsymbol{x}(t)$ describes the deviation of the perturbed trajectory from the reference trajectory $\boldsymbol{x}(t)$ at time t, and it is understood that $\delta\boldsymbol{x}(t_I) = \delta\boldsymbol{x}(t_F) = \boldsymbol{0}$ Now we have

$$\delta\Phi(\boldsymbol{x}, t) = \delta\boldsymbol{x} \cdot \nabla_{\boldsymbol{x}}\Phi(\boldsymbol{x}, t) = -\delta\boldsymbol{x} \cdot \boldsymbol{F}(\boldsymbol{x}, t) = -\delta\boldsymbol{x} \cdot m\,\ddot{\boldsymbol{x}}$$

The velocity and acceleration for the perturbed trajectory $\boldsymbol{x} + \delta\boldsymbol{x}$ are $\dot{\boldsymbol{x}} + \delta\dot{\boldsymbol{x}}$ and $\ddot{\boldsymbol{x}} + \delta\ddot{\boldsymbol{x}}$ such that

$$\frac{\mathrm{d}}{\mathrm{d}t}\left(m\,\dot{\boldsymbol{x}} \cdot \delta\boldsymbol{x}\right) = m\,\ddot{\boldsymbol{x}} \cdot \delta\boldsymbol{x} + m\,\dot{\boldsymbol{x}} \cdot \delta\dot{\boldsymbol{x}} = m\,\ddot{\boldsymbol{x}} \cdot \delta\boldsymbol{x} + \delta\frac{m\,\dot{\boldsymbol{x}}^2}{2}$$

where $T = m\,\dot{\boldsymbol{x}}^2/2$ is the kinetic energy. Hence, we can express the variation of the potential as

$$\begin{aligned} \delta\Phi(\boldsymbol{x}, t) &= -\frac{\mathrm{d}}{\mathrm{d}t}\left(\delta\boldsymbol{x} \cdot m\,\dot{\boldsymbol{x}}\right) + \delta T(\dot{\boldsymbol{x}}) \\ \Rightarrow \quad \delta\big(T(\dot{\boldsymbol{x}}) - \Phi(\boldsymbol{x}, t)\big) &= -\frac{\mathrm{d}}{\mathrm{d}t}\left(\delta\boldsymbol{x} \cdot m\,\dot{\boldsymbol{x}}\right) \end{aligned}$$

The difference between the kinetic and potential energy is a total time derivative. Integrating the expression over time from t_I to t_F therefore provides

$$\int_{t_I}^{t_F} \mathrm{d}t\, \delta\big(T(\dot{\boldsymbol{x}}) - \Phi(\boldsymbol{x}, t)\big) = -\int_{t_I}^{t_F} \mathrm{d}t\, \frac{\mathrm{d}}{\mathrm{d}t}\left(\delta\boldsymbol{x} \cdot m\,\dot{\boldsymbol{x}}\right) \tag{6.2.1}$$

$$= \delta\boldsymbol{x}(t_I) \cdot m\,\dot{\boldsymbol{x}}(t_I) - \delta\boldsymbol{x}(t_F) \cdot m\,\dot{\boldsymbol{x}}(t_F) = 0 \tag{6.2.2}$$

The integral vanishes because $\boldsymbol{x}$ is fixed a the start and the end point.

Up to mathematical identities that are always true we only used Newton's law $\boldsymbol{F}(\boldsymbol{x}, t) = m\ddot{\boldsymbol{x}}$ to arrive at this conclusion. This observation is denoted as the principle of least action. Rather than on

Newton axioms we may therefore base mechanics on the principle of least action.

Definition 6.3: Lagrangian

We consider a dynamics with kinetic energy $T(\dot{\boldsymbol{x}}(t))$ and potential energy $\Phi(\boldsymbol{x}(t), t)$ for trajectories $\boldsymbol{x}(t)$. The difference

$$\mathcal{L}(\boldsymbol{x}, \dot{\boldsymbol{x}}, t) = T(\dot{\boldsymbol{x}}) - \Phi(\boldsymbol{x}, t)$$

will be called *Lagrangian* or *Lagrange function* of the dynamics.

Definition 6.4: Action of a trajectory

For a dynamics with Lagrangian $\mathcal{L}(\boldsymbol{x}, \dot{\boldsymbol{x}}, t)$ the *action* $S[\boldsymbol{x}(t), \dot{\boldsymbol{x}}(t)]$ of a trajectory $\boldsymbol{x}(t)$, $t_I \leq t \leq t_F$ with velocity $\dot{\boldsymbol{x}}(t)$ is defined as

$$S[\boldsymbol{x}(t), \dot{\boldsymbol{x}}(t)] = \int_{t_I}^{t_F} \mathrm{d}t\, \mathcal{L}(\boldsymbol{x}(t), \dot{\boldsymbol{x}}(t), t)$$

The *variation of the action* will be defined as

$$\delta S[\boldsymbol{x}(t), \dot{\boldsymbol{x}}(t)] = \int_{t_I}^{t_F} \mathrm{d}t\, \delta\mathcal{L}(\boldsymbol{x}(t), \dot{\boldsymbol{x}}(t), t)$$

Axiom 6.1: Principle of least action

Let $\boldsymbol{x}(t)$ with $t_I \leq t \leq t_F$ be a trajectory from $\boldsymbol{x}(t_I)$ to $\boldsymbol{x}(t_F)$ that satisfies Newton's law $\boldsymbol{F}(\boldsymbol{x}, t) = m\ddot{\boldsymbol{x}}$ with a force that is derived from a potential $\Phi(\boldsymbol{x}, t)$. The the variation of the action associated the trajectory will vanish

$$0 = \delta S[\boldsymbol{x}(t), \dot{\boldsymbol{x}}(t)]$$

Remark 6.1. The principle is called *least* action principle. However, it only requires that the action has a critical point. There are many examples in physics where the action takes a saddle point, rather than a minimum.

The principle provides an alternative way to determine EOM that proceeds as follows.

$$\begin{aligned} 0 = \delta S[\boldsymbol{x}(t), \dot{\boldsymbol{x}}(t)] &= \int_{t_I}^{t_F} \mathrm{d}t\, \delta\mathcal{L}(\boldsymbol{x}(t), \dot{\boldsymbol{x}}(t), t) \\ &= \int_{t_I}^{t_F} \mathrm{d}t\, \left[\delta\dot{\boldsymbol{x}}\, \nabla_{\dot{\boldsymbol{x}}}\mathcal{L}(\boldsymbol{x}, \dot{\boldsymbol{x}}, t) + \delta\boldsymbol{x}\, \nabla_{\boldsymbol{x}}\mathcal{L}(\boldsymbol{x}, \dot{\boldsymbol{x}}, t)\right] \\ &= \int_{t_I}^{t_F} \mathrm{d}t\, \delta\boldsymbol{x}\, \left[\left(-\frac{\mathrm{d}}{\mathrm{d}t}\nabla_{\dot{\boldsymbol{x}}}\mathcal{L}(\boldsymbol{x}, \dot{\boldsymbol{x}}, t)\right) + \nabla_{\boldsymbol{x}}\mathcal{L}(\boldsymbol{x}, \dot{\boldsymbol{x}}, t)\right] \end{aligned}$$

In the last step we performed a partial integration.[1] The integral must vanish for every choice of the variation $\delta\boldsymbol{x}$. In particular we may choose a function $\delta\boldsymbol{x}$ that takes the same sign as the square bracket whenever it does not vanish. However, in that case the

[1] The boundary term of the partial integration vanishes,

$$\begin{aligned} \left[\delta\boldsymbol{x}\, \nabla_{\dot{\boldsymbol{x}}}\mathcal{L}(\boldsymbol{x}, \dot{\boldsymbol{x}}, t)\right]_{t_I}^{t_F} &= \delta\boldsymbol{x}(t_F)\ \left[\nabla_{\dot{\boldsymbol{x}}}\mathcal{L}(\boldsymbol{x}, \dot{\boldsymbol{x}}, t)\right]_{t=t_F} \\ &\quad - \delta\boldsymbol{x}(t_I)\ \left[\nabla_{\dot{\boldsymbol{x}}}\mathcal{L}(\boldsymbol{x}, \dot{\boldsymbol{x}}, t)\right]_{t=t_F} \\ &= 0 \end{aligned}$$

integral is strictly positive unless the square bracket vanishes. This provides the EOM of the dynamics in terms of the Euler-Lagrange equation.

Theorem 6.1: Euler-Lagrange equations

Let $x_i(t)$ be a coordinates of a trajectory $\boldsymbol{x}(t)$ of a dynamics with Lagrangian $\mathcal{L}(\boldsymbol{x}, \dot{\boldsymbol{x}}, t)$. Then $x_i(t)$ is a solution of the *Euler-Lagrange equation*

$$\frac{\mathrm{d}}{\mathrm{d}t} \frac{\partial}{\partial \dot{x}_i} \mathcal{L}(\boldsymbol{x}, \dot{\boldsymbol{x}}, t) = \frac{\partial}{\partial x_i} \mathcal{L}(\boldsymbol{x}, \dot{\boldsymbol{x}}, t) \tag{6.2.3}$$

6.2.2 *Euler-Lagrange equations for generalized coordinates*

The Euler-Lagrange equations derive from a variational principle that states that the gradient of the Lagrange function with respect to the phase-space coordinate $\boldsymbol{\Gamma} = (\boldsymbol{x}, \dot{\boldsymbol{x}})$ must vanish for physically admissible trajectories. This holds for *all* directions in phase space. However, generalized coordinates do not qualify as a vector such that some care is needed to derive their EOM.

Let $\boldsymbol{q}$ be the generalized coordinates of a system and $\boldsymbol{x}(\boldsymbol{q})$ the associated configuration vector of the system. Note that $\boldsymbol{x}$ is a vector with all properties discussed in Chapter 2, while $\boldsymbol{q}$ might only be a tuple of functions that provide a convenient parameterization of valid configurations. We address the situation where the forces in the system are conservative, arising from a potential energy $\Phi\big(\boldsymbol{x}(\boldsymbol{q}), t\big)$. Moreover, we assume the the potential energy can be split into a part $\Phi_c\big(\boldsymbol{x}(\boldsymbol{q}), t\big)$ that accounts for the forces that constraint the motion of the system, and a part $U\big(\boldsymbol{x}(\boldsymbol{q}), t\big)$ that accounts for all other forces.

Example 6.3: Rollercoaster trail

The position $\boldsymbol{x}(t)$ on the trail of a rollercoaster can uniquely be described by the (dimensionless) distance ℓ along the trail that it has gone. Hence, generalized coordinate $\ell(t)$ uniquely describes the configuration $\boldsymbol{x}(\ell(t))$ of the rollercoaster at time t.

Example 6.4: Driven pendulum

A driven pendulum is a mathematical pendulum where the position of the fulcrum $\boldsymbol{X}_f$ and the length of the pendulum arm $L(t)$ are subjected to a prescribed temporal evolution. The position of the pendulum weight, $\boldsymbol{x}$, may then be described by the angle $\theta \in [0, 2\pi] = \mathbb{D}$,

$$\boldsymbol{x}(\theta, t) = \boldsymbol{X}_f(t) + R(t) \begin{pmatrix} \cos\theta \\ \sin\theta \end{pmatrix}$$

Here, the time dependence of $\boldsymbol{X}_f(t)$ and $R(t)$ reflect the temporal evolution of the time-dependent setup of the pendulum. The temporal evolution of the pendulum will be described in terms of the generalized coordinate $\theta(t)$.

We will now explore the implications of the principle of least actions for variations of the path that refer only to accessible coordinates. For the $k$the coordinate of the variation we write

$$\delta x_k = x_k(\boldsymbol{q} + \delta \boldsymbol{q}, t) - x_k(\boldsymbol{q}, t) = \sum_{\nu=1}^{d} \frac{\partial x_k}{\partial q_\nu}\, \delta q_\nu$$

and for the associated time derivative we have

$$\delta \dot{x}_k = \frac{\mathrm{d}}{\mathrm{d}t} \delta x_k = \sum_{\nu=1}^{d} \frac{\partial \dot{x}_k}{\partial q_\nu}\, \delta q_\nu + \sum_{\nu=1}^{d} \frac{\partial x_k}{\partial q_\nu}\, \delta \dot{q}_\nu$$

As a consequence the variation of the Lagrangian takes the form

$$\delta \mathcal{L} = \delta \boldsymbol{x} \cdot \nabla_{\boldsymbol{x}} \mathcal{L} + \delta \dot{\boldsymbol{x}} \cdot \nabla_{\dot{\boldsymbol{x}}} \mathcal{L} = \delta \boldsymbol{x} \cdot (\boldsymbol{F}_c + \boldsymbol{F}_e) + \delta \dot{\boldsymbol{x}} \cdot m \dot{\boldsymbol{x}}$$

where $\boldsymbol{F}_c$ represent the constraint forces. We consider variations $\delta \boldsymbol{x}$ that relate trajectories complying with the constraints such that $\delta \boldsymbol{x} \cdot \boldsymbol{F}_c = 0$. Therefore, in the setting of generalized coordinates one need not account for constraint forces. We will now express the variation of the Lagrangian in terms of the variations of the generalized coordinates,

$$\begin{aligned}
\delta \mathcal{L} &= \sum_{k=1}^{D} \left[\delta x_k \frac{\partial \mathcal{L}}{\partial x_k} + \delta \dot{x}_k \frac{\partial \mathcal{L}}{\partial \dot{x}_k} \right] \\
&= \sum_{k=1}^{D} \left[\left(\sum_{\nu=1}^{d} \frac{\partial x_k}{\partial q_\nu}\, \delta q_\nu \right) \frac{\partial \mathcal{L}}{\partial x_k} + \sum_{\nu=1}^{d} \left(\frac{\partial \dot{x}_k}{\partial q_\nu}\, \delta q_\nu + \frac{\partial x_k}{\partial q_\nu}\, \delta \dot{q}_\nu \right) \frac{\partial \mathcal{L}}{\partial \dot{x}_k} \right] \\
&= \sum_{\nu=1}^{d} \delta q_\nu \sum_{k=1}^{D} \left(\frac{\partial x_k}{\partial q_\nu} \frac{\partial \mathcal{L}}{\partial x_k} + \frac{\partial \dot{x}_k}{\partial q_\nu} \frac{\partial \mathcal{L}}{\partial \dot{x}_k} \right) + \sum_{\nu=1}^{d} \delta \dot{q}_\nu \sum_{k=1}^{D} \frac{\partial x_k}{\partial q_\nu} \frac{\partial \mathcal{L}}{\partial \dot{x}_k}
\end{aligned}$$

On the other hand

$$\begin{aligned}
\frac{\partial \mathcal{L}(\boldsymbol{x}(\boldsymbol{q}, t), \dot{\boldsymbol{x}}(\boldsymbol{q}, \dot{\boldsymbol{q}}, t), t)}{\partial q_\nu} &= \sum_{k=1}^{D} \left(\frac{\partial x_k}{\partial q_\nu} \frac{\partial \mathcal{L}}{\partial x_k} + \frac{\partial \dot{x}_k}{\partial q_\nu} \frac{\partial \mathcal{L}}{\partial \dot{x}_k} \right) \\
\frac{\partial \mathcal{L}(\boldsymbol{x}(\boldsymbol{q}, t), \dot{\boldsymbol{x}}(\boldsymbol{q}, \dot{\boldsymbol{q}}, t), t)}{\partial \dot{q}_\nu} &= \sum_{k=1}^{D} \frac{\partial \mathcal{L}(\boldsymbol{x}(\boldsymbol{q}, t), \dot{\boldsymbol{x}}(\boldsymbol{q}, \dot{\boldsymbol{q}}, t), t)}{\partial \dot{x}_k} \frac{\partial \dot{x}_k}{\partial \dot{q}_\nu} \\
&= \sum_{k=1}^{D} \frac{\partial \mathcal{L}}{\partial \dot{x}_k} \frac{\partial}{\partial \dot{q}_\nu} \left(\frac{\partial x_k}{\partial t} + \sum_{\mu=1}^{d} \frac{\partial x_k}{\partial q_\mu}\, \dot{q}_\mu \right) \\
&= \sum_{k=1}^{D} \frac{\partial \mathcal{L}}{\partial \dot{x}_k} \frac{\partial x_k}{\partial q_\nu}
\end{aligned}$$

Therefore,

$$\begin{aligned}
\delta S &= \int \mathrm{d}t \delta \mathcal{L} = \int \mathrm{d}t \sum_{\nu=1}^{d} \left(\delta q_\nu \frac{\partial \mathcal{L}}{\partial q_\nu} + \delta \dot{q}_\nu \frac{\partial \mathcal{L}}{\partial \dot{q}_\nu} \right) \\
&= \int \mathrm{d}t \sum_{\nu=1}^{d} \delta q_\nu \left(\frac{\partial \mathcal{L}}{\partial q_\nu} - \frac{\mathrm{d}}{\mathrm{d}t} \frac{\partial \mathcal{L}}{\partial \dot{q}_\nu} \right)
\end{aligned}$$

The equations of motion are derived from the Lagrangian, Definition 6.5, by Algorithm 6.1.

Definition 6.5: Lagrangian in generalized coordinates

The Lagrange function $\mathcal{L}$ amounts to the difference of the kinetic energy T and the potential energy U of the system,

$$\mathcal{L} = T - U = \sum_\alpha \frac{m_\alpha}{2} \dot{x}_\alpha^2(\boldsymbol{q}) - U\big(\boldsymbol{x}(\boldsymbol{q})\big) \tag{6.2.4}$$

Constraint forces are not considered.

Algorithm 6.1: Euler Lagrange EOMs

a) Identify generalized coordinates $\boldsymbol{q}$ that describe the admissible configurations of the system.

b) Determine $\boldsymbol{x}(\boldsymbol{q})$, and the resulting expression of the potential energy in terms of $\boldsymbol{q}$,

$$U(\boldsymbol{q}) = U\big(\boldsymbol{x}(\boldsymbol{q})\big)$$

c) Evaluate the kinetic energy based on the chain rule

$$T(\boldsymbol{q}, \dot{\boldsymbol{q}}) = \sum_\alpha \frac{m_\alpha}{2} \dot{x}_\alpha^2(\boldsymbol{q}) = \sum_\alpha \frac{m_\alpha}{2} \left(\sum_i \frac{\partial x_\alpha}{\partial q_i} \, \dot{q}_i \right)^2$$

where x_α is the α-component of the configuration vector $\boldsymbol{x}$ and m_α the mass of the associated particle.

Hence, we establish the Lagrange function

$$\mathcal{L}(\boldsymbol{q}, \dot{\boldsymbol{q}}) = T(\boldsymbol{q}, \dot{\boldsymbol{q}}) - U(\boldsymbol{q})$$

expressed in terms of the generalized coordinates $\boldsymbol{q}$ and their time derivatives $\dot{\boldsymbol{q}}$.

d) Determine the EOM for the component q_i of $\boldsymbol{q}$ by evaluating the *Euler-Lagrange equation*

$$\frac{\mathrm{d}}{\mathrm{d}t} \frac{\partial \mathcal{L}}{\partial \dot{q}_i} = \frac{\partial \mathcal{L}}{\partial q_i} \tag{6.2.5}$$

6.3 *Dynamics with one degree of freedom*

We will now illustrate the application of the Lagrange formalism for three examples with a single degree of freedom of the motion: The mathematical pendulum, Example 6.1, will give a first idea of how to find EOMs with the Lagrange formalism. This EOM can also easily be found by other approaches. 2. The motion of a pearl on a rotating ring constitutes a system with an explicit time dependence. In that case the Lagrange formalism dramatically simplifies the the derivation of the EOM. We will also discuss for this model how to account for dissipative forces and we will see how the solutions of a problem can change qualitatively upon varying a parameter. 3. The motion of a weight on a carousel we will discussed as an example of a system that needs a dedicated treatment for the description of admissible positions.

6.3.1 *The EOM for the mathematical pendulum*

The parameterization introduced in Example 6.1 provides the kinetic energy

$$T = \frac{M}{2}\,\dot{\boldsymbol{x}}^2 = \frac{M}{2}\,L^2\,\dot\theta^2\,\hat{\boldsymbol{\theta}}(\theta(t))^2 = \frac{M}{2}\,L^2\,\dot\theta^2$$

and the potential energy in the gravitational field

$$U = -M\boldsymbol{g}\cdot\boldsymbol{x} = -M\,L\,\hat{\boldsymbol{R}}\big(\theta(t)\big)\cdot\boldsymbol{g} = -M\,L\,g\cos\theta(t)$$

since $\boldsymbol{g} = g\,\hat{\boldsymbol{R}}(0)$.

Consequently,

$$\begin{aligned}
\mathcal{L} &= \frac{M}{2}\,L^2\,\dot\theta^2 + M\,g\,L\,\cos\theta(t)\\
\Rightarrow\quad M\,L^2\,\ddot\theta(t) &= \frac{\mathrm{d}}{\mathrm{d}t}\frac{\partial\mathcal{L}}{\partial\dot\theta} = \frac{\partial\mathcal{L}}{\partial\theta} = -M\,g\,L\,\sin\theta(t)\\
\Rightarrow\quad \ddot\theta(t) &= -\frac{g}{L}\,\sin\theta(t)
\end{aligned}\tag{6.3.1}$$

The EOM (6.3.1) can be integrated once by multiplication with $2\dot\theta(t)$

$$\begin{aligned}
\dot\theta^2(t) - \dot\theta^2(t_0) &= \int_{t_0}^{t}\mathrm{d}t\,2\dot\theta\ddot\theta = \int_{t_0}^{t}\mathrm{d}t\,2\dot\theta\left(-\frac{g}{L}\,\sin\theta(t)\right)\\
&= 2\int_{\theta(t_0)}^{\theta(t)}\mathrm{d}\theta\,\frac{\mathrm{d}}{\mathrm{d}\theta}\left(\frac{g}{L}\,\cos\theta\right) = 2\,\frac{g}{L}\,\big(\cos\theta(t) - \cos\theta(t_0)\big)
\end{aligned}$$

This is a Mattheiu differential equation. For most initial conditions it can not be solved by simple means. However, the first integral provides the phase-space trajectories $\dot\theta(\theta)$ for every given set of initial conditions $\big(\theta(t_0),\dot\theta(t_0)\big)$,

$$\dot\theta = \pm\sqrt{\dot\theta^2(t_0) + \frac{2\,g}{L}\,\big(\cos\theta(t) - \cos\theta(t_0)\big)}$$

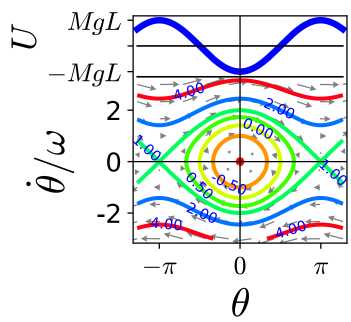

Figure 6.4: The potential $U(\theta)$ (top) and the phase-space plot (bottom) for the EOM (6.3.1) of the mathematical pendulum. The numbers marked on the contour lines indicated the energy of a trajectory in units of MgL.

The phase-space portrait is shown in Figure 6.4. There are trivial solutions where the pendulum is resting without motion at its stable and unstable rest positions $\theta = 0$ and $\theta = \pi$, These positions are denoted as *fixed points* of the dynamics. There are closed circular trajectories close to the minimum, $\theta = 0$, of the potential where it is harmonic to a good approximation. These are solutions with energies $0 < 1 + E/MgL \lesssim 1$.

For larger amplitudes the amplitude of the swinging grows, and the circular trajectories get deformed. When E approaches MgL the phase-space trajectories arrive close to the tipping points $\theta = \pm\pi$ where they form very sharp edges. For θ close to $\theta = \pm\pi$ the trajectories look like the hyperbolic scattering trajectories for the potential $-a\,x^2/2$ that was discussed in Problem 4.25. When the non-dimensional energy is exactly one, the pendulum starts on top, goes through the minimum and returns to the top again. Apart from the fixed points, this is the only case where the evolution can be obtained in terms of elementary functions. For the initial condition $\dot\theta(t_i) = 0$ and $\cos\theta_i = -1$ we find

$$\omega^{-1}\,\dot\theta_H(t) = \pm\sqrt{2 + 2\,\cos\theta_H(t)} = \pm 2\,\cos\frac{\theta_H(t)}{2}$$

The same equation is also obtained for the initial condition $\theta_0 = 0$ and $\dot\theta(t_0) = \sqrt{2g/L}$ half-way on the way from the top back to the top. For this initial condition the ODE for $\dot\theta_H$ can be integrated, and we find

$$\pm 2\,\omega\,(t - t_0) = \int_0^{\theta(t)} \frac{\mathrm{d}\theta}{\cos\frac{\theta}{2}} = \ln\frac{1 + \sin\frac{\theta_H(t)}{2}}{1 - \sin\frac{\theta_H(t)}{2}} - \ln\frac{1}{1}$$

$$\Rightarrow \qquad \theta_H(t) = 2\,\arcsin\tanh\big(\pm\omega\,t\big) \tag{6.3.2}$$

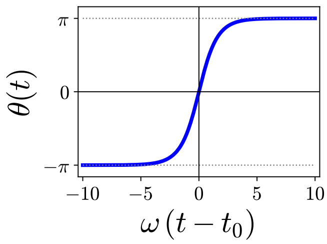

Figure 6.5: Anticlockwise moving heterocline for the mathematical pendulum.

The $\pm$ signs account for the possibility that the pendulum can move clockwise and counterclockwise. The counterclockwise trajectory is shown in Figure 6.5. In the limit $t \to -\infty$ it starts in the unstable fixed point $\theta = -\pi$. It falls down till it reaches the minimum $\theta = 0$ at time t_0, and then it rises again, reaching the maximum $\theta = \pi$ for time $t \to \infty$. Such a trajectory is called a homocline.

Definition 6.6: Homoclines and Heteroclines

Homoclines and *heteroclines* are trajectories that approach a fixed points of a dynamics in their infinite past and future. A homocline returns to the same fixed point from where it started. A heterocline connects two different fixed points.

The take-home message of this example is that the minima and maxima of a potential organize the phase space flow. Close to each minimum a conservative system will have closed trajectories that represent oscillations in a potential well. The well is confined by maxima to the left and right of the minimum of the potential. When these maxima have different height there is a homoclinic orbit coming down from and returning to the shallower maximum. When they have the same height, they are connected by heteroclinic orbits. Thus, the homoclines and heteroclines divide the phase space into different domains. Initial conditions within the same domain show qualitatively similar dynamics. Initial conditions in different domains feature different dynamics. For the mathematical pendulum the heteroclines divide are three domains, up to the 2π translation symmetry of θ:

a) There are trajectories oscillating around $\theta = 0$, with energies smaller than MgL. The region of these oscillations is bounded by the heteroclines provided in Equation (6.3.2).

b) Trajectories with initial conditions lying above the anticlockwise moving heterocline will persistently rotate anticlockwise and never reverse their motion.

c) Trajectories with initial conditions lying below the clockwise moving heterocline will persistently rotate clockwise and never reverse their motion.

The general strategy for sketching phase-space plots is summarized in the following algorithm.

Algorithm 6.2: Phase space plots

a) Identify the minima and maxima of the potential. Mark the minima as (marginally) stable fixed points with velocity zero. Mark the maxima as unstable fixed points with velocity zero.

b) Identify the fate of trajectories departing from the unstable fixed points. Identify to this end the closest positions on the potential that have the same height as the maximum. When it is another extremum the orbit will form an heterocline. Otherwise, it will be reflected and return to the initial maximum, forming a homocline. If there is no further point of the same height, the trajectory will escape to infinity.

c) Add characteristic trajectories close to the minima and in between homo- and heteroclines.

d) Observe the symmetries of the system. To the very least the plot is symmetric with respect to reflection at the horizontal axis, i. e. swapping the sign of the velocity.

e) Observe energy conservation (if it applies): The modulus of the velocity takes a local minimum for a maximum of the potential, and a local maximum for a minimum of the potential.

6.3.2 *The EOM for a pearl on a rotating ring*

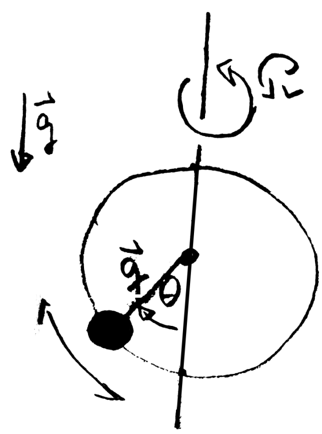

Figure 6.6: Motion of a pearl moving on a ring rotating with a fixed frequency Ω.

We consider a pearl of mass M that can freely move on a ring. The ring is mounted vertically in the gravitational field and it spins with angular velocity Ω around its vertical symmetry axis. Again the setup constraints the position of the pearl to lie on a spherical shell, and we hence describe its position as

$$\boldsymbol{x}(t) = \ell\, \hat{\boldsymbol{R}}\big(\theta(t), \phi(t)\big)$$

However, in this case the position of the pearl is fully described by the angle $\theta(t)$ of the deflection of the pearl from the direction of gravity (see Figure 6.6. The angle $\phi(t) = \Omega t$ is entering the

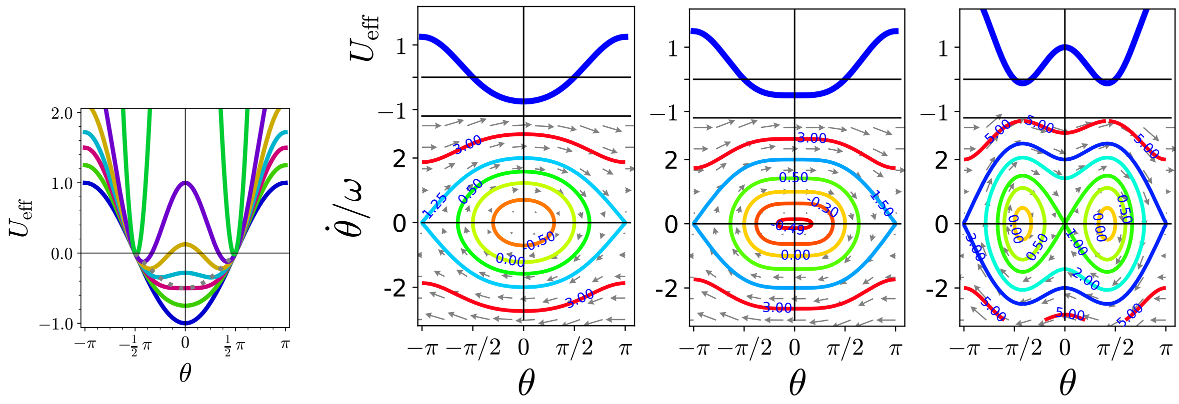

Figure 6.7: The left panel shows the effective potential for the pearl on a ring for parameter values $(\Omega/\omega) \in \{0, 2^{-1/2}, 1, 1.2, 1.5, 2, 5\}$ from bottom to top. The subsequent panels show phase-space portraits of the motion for $\Omega/\omega = 2^{-1/2}$, 1, and 2, respectively.

problem as a parameter, dictated by the setup of the problem, and the motion of the pearl on the ring will be described based on a single EOMs for its coordinate $\theta(t)$.

The potential energy takes the same form as for the pendulum,

$$U = -M\,\boldsymbol{g} \cdot \boldsymbol{x} = -M\,g\,\ell\,\cos\theta(t)\,.$$

The kinetic energy is obtained based on its velocity

$$\dot{\boldsymbol{x}} = \ell\,\dot\theta\,\hat{\boldsymbol{\theta}}(\theta(t), \Omega t) + \ell\,\Omega\,\sin\theta(t)\,\hat{\boldsymbol{\phi}}(\theta(t), \Omega t)$$

which provides the Lagrange function

$$\mathcal{L}(\theta, \dot\theta) = \frac{M}{2}\,\ell^2\,\dot\theta^2 + \frac{M}{2}\,\ell^2\,\Omega^2\,\sin^2\theta(t) + M\,g\,\ell\,\cos\theta(t)$$

It only differs from the expression for the spherical pendulum by the fact that $\phi(t)$ is not a coordinate whose evolution must be determined from an EOM. Rather it is a parameter $\phi(t) = \Omega\,t$ provided by the setting of the problem.

The motion only has a single DOF, $\theta(t)$, with EOM

$$\ddot\theta(t) = -\frac{g}{\ell}\,\sin\theta(t)\,\left(1 - \frac{\ell\,\Omega^2}{g}\,\cos\theta(t)\right) \tag{6.3.3}$$

This EOM can once be integrated by the same strategy adopted for the swing and the spherical pendulum. Thus, one finds the effective potential

$$U_{\text{eff}}(\theta) = -\omega^2\,\cos\theta\,\left[1 - \frac{1}{2}\,\left(\frac{\Omega}{\omega}\right)^2\,\cos\theta\right]$$

Figure 6.7 shows the effective potential and phase space portraits for different values of angular momentum, i. e. of the dimensionless control parameter $\kappa = \Omega/\omega$. For $\kappa < 1$ the phase space has the same structure as that of a planar mathematical pendulum, with a stable fixed point at $\theta = 0$. When κ passes through one, this minimum of U_{eff} turns into a maximum, and two new minima emerge at the positions $\theta_c = \pm \arccos \kappa^{-2}$ that are indicated by a dotted gray line in the left panel of Figure 6.7. The new maximum at zero is always shallower than the maxima at $\pm\pi$. Hence, it gives rise to two homoclinic orbit that wind around the new stable fixed points. The maxima at $\pm\pi$ will further we connected by heteroclinic orbits. Hence, phase space is divided into five distinct regions. For energies smaller than $U_{\text{eff}}(\theta = 0)$ the trajectories wiggle around one of the stable fixed points. They stay on one side of the ring and oscillate around the angle θ_c. There are two regions of this type because the pear can stay on both sides of the ring. For $U_{\text{eff}}(\theta = 0) < E < U_{\text{eff}}(\theta = \pi)$ the trajectories show oscillations back and forth between the two sides of the ring, For $E > U_{\text{eff}}(\theta = \pi)$ they rotate around the ring in clockwise or counter-clockwise direction for $\dot\theta < 0$ or $\dot\theta > 0$, respectively.

There are two take-home message from this example:

1. There are no conservation laws in the dynamics when there are explicitly time-dependent constraints. Hence, the strategies of Chapter 4 to establish and discuss the EOM can no longer be applied. However, the Lagrange formalism still provides the EOM in a straightforward manner.

2. In general, the structure of the phase-space flow changes upon varying the dimensionless control parameters of the dynamics. These changes are called bifurcations, and they are a very active field of contemporary research in theoretical mechanics. The pearl on the ring features a pitchfork bifurcation since the positions of the fixed points resemble the shape of a pitch fork (see Figure 6.8). We will come back to this topic in due time.

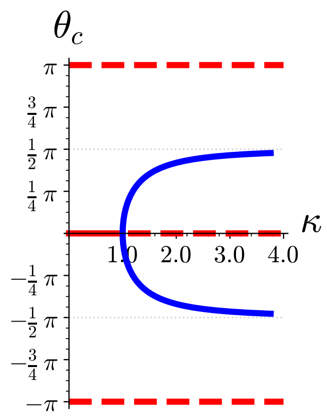

Figure 6.8: Parameter dependence of the positions of the fixed points of the rotation governor. Solid lines mark stable fixed points, and unstable fixed points are marked by dashed lines.

6.3.3 *Centrifugal Governor*

In the absence of rotation the motion of the pearl on the ring amounts to a mathematical pendulum with frequency ω. This relation is used in centrifugal governors that are used to control the rotation of mills and steam engines. The sharp increase of θ_c when the rotation frequency rises beyond Ω is used in a feedback mechanism of the governor to control for instance the rotation speed of the steam engine.

Oscillations around the stable fixed points is an undesirable feature in the governor such that some dissipation is a welcome feature of the governor. We revisit Equation (6.2.1) to extend the Lagrange formalism for forces that do not derive from a potential

$$
\begin{aligned}
0 &= -\int_{t_I}^{t_F} \mathrm{d}t\, \frac{\mathrm{d}}{\mathrm{d}t} \left(\delta \boldsymbol{x} \cdot m\, \dot{\boldsymbol{x}}\right) = -\int_{t_I}^{t_F} \mathrm{d}t\, \left(\delta\dot{\boldsymbol{x}} \cdot m\, \dot{\boldsymbol{x}} + \delta\boldsymbol{x} \cdot m\, \ddot{\boldsymbol{x}}\right) \\
&= -\int_{t_I}^{t_F} \mathrm{d}t\, \left(\delta\dot{\boldsymbol{x}} \cdot \nabla_{\dot{\boldsymbol{x}}} \mathcal{L} + \delta\boldsymbol{x} \cdot m \left(\boldsymbol{F}_d - \nabla_{\boldsymbol{x}} \Phi\right)\right) \\
&= \int_{t_I}^{t_F} \mathrm{d}t\, \delta\boldsymbol{x} \left(-\boldsymbol{F}_d + \nabla_{\boldsymbol{x}} \mathcal{L} - \frac{\mathrm{d}}{\mathrm{d}t} \nabla_{\dot{\boldsymbol{x}}} \mathcal{L}\right)
\end{aligned}
$$

Thus, and additional dissipative force $\boldsymbol{F}_d = -\gamma\, \dot\theta\, \hat{\boldsymbol{\theta}}$ will give rise to an additional additive term in Equation (6.3.3) such that the

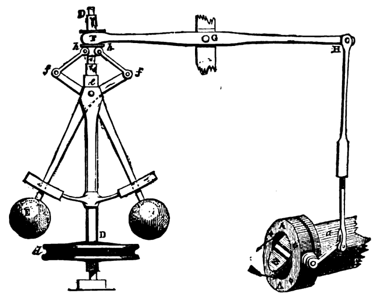

Figure 6.9: Rotational governor and throttle valve. When the rotation speed exceeds a critical value the weights move outward and the arm opens a valve that reduces pressure in the steam engine. (Image from "Discoveries & Inventions of the Nineteenth Century" by R. Routledge, 13th edition, published 1900, Public domain, via Wikimedia Commons)

rotational governor has an EOM

$$\ddot{\theta}(t) = -\frac{g}{\ell}\,\sin\theta(t)\,\left(1 - \frac{\ell\,\Omega^2}{g}\,\cos\theta(t)\right) - \frac{\gamma}{M}\,\dot{\theta}(t)$$

and the energy evolves as

$$\frac{\mathrm{d}}{\mathrm{d}t}\left(\frac{\dot{\theta}^2}{2} + U_{\text{eff}}(\theta)\right) = -\frac{\gamma}{M}\,\dot{\theta}^2(t)$$

Small friction deflects the trajectories towards smaller values of the effective potential, until the system comes to rest in a stable fixed point. The impact of dissipation for $\Omega/\omega = 2$ and dissipation of $\gamma/M = 0.2$ and 2.0, respectively are shown in Figure 6.10.

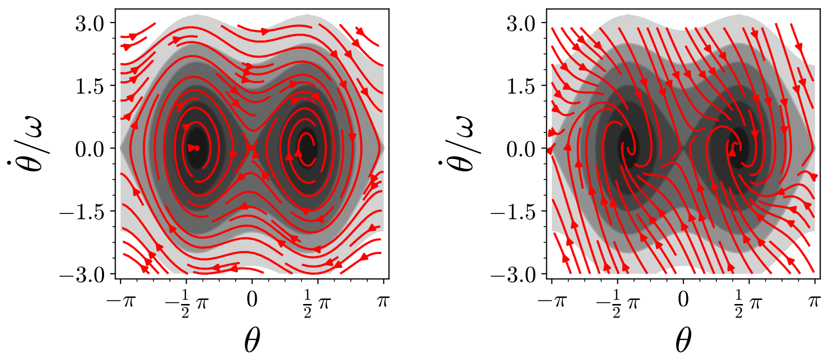

Figure 6.10: Phase-space plot for a rotational governor with rotation frequency $\Omega = 2\omega$. The colors of gray in the background show contour levels of the energy. The streamlines indicated the evolution of the dynamics for (left) weak dissipation, $\gamma = 0.2$, and (right) strong dissipation, $\gamma = 2$, dissipation. Due to dissipation the trajectories acquire a component downwards in energy.

6.3.4 *Carousel*

The positions in the systems that we treated so far could be described in terms of polar and spherical coordinates. Commonly the parameterization of particle configurations needs a dedicated treatment. As an example for such a problem we treat the motion of the beats of a toy carousel that is shown in Figure 6.11. The carousel is composed of four cantilever beams of length R that extend outwards from a vertical axis that is rotating with angular velocity Ω. At the far end of each beam there is a pendulum attached that freely swings in outward direction. Their inclination towards gravity will be denoted as θ. (Oscillations parallel to the motion will not be considered for the time being.) The pendulum arm has a length L and it carries a weight m. Due to a magnetic contact the pendulum experiences minimal friction in its motion. Henceforth the focus on the motion of one of the beats.

We pick the origin of the coordinate system on the ration axes right on the height of the cantilever. Looking from the top (right panel of Figure 6.11) the pendulum arm sticks out in direction $\phi = \Omega t$. Adopting polar coordinates in the horizontal plane, we thus denote the position of the fulcrum of the pendulum as $\boldsymbol{R} = R\,\hat{\boldsymbol{r}}(\phi)$,

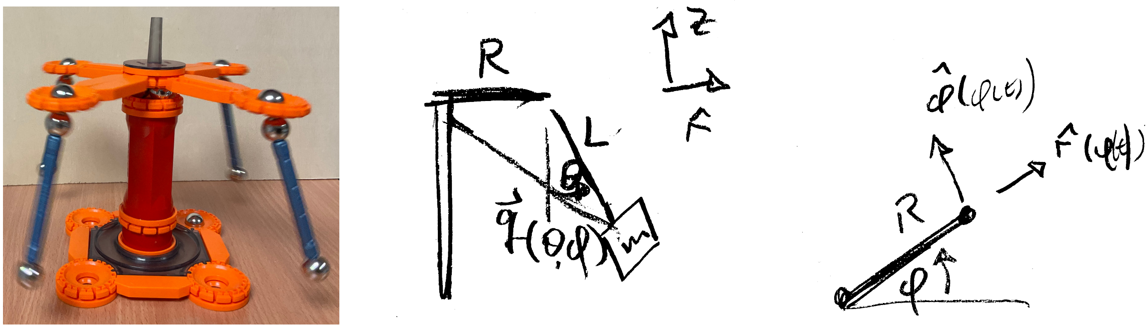

Figure 6.11: Experimental setup and description of configurations for a toy carousel.

and the vector from the fulcrum to the weight is $L\,\sin\theta\,\hat{\boldsymbol{r}}(\phi) - L\,\cos\theta\,\hat{\boldsymbol{z}}$. Thus, the position $\boldsymbol{x}$ and the velocity $\dot{\boldsymbol{x}}$ of the weight are

$$\begin{aligned}\boldsymbol{x} &= (R + L\,\sin\theta)\,\hat{\boldsymbol{r}}(\Omega t) - L\,\cos\theta\,\hat{\boldsymbol{z}}\\ \dot{\boldsymbol{x}} &= (R + L\,\sin\theta)\,\Omega\,\hat{\boldsymbol{\phi}}(\Omega t) + L\,\cos\theta\,\dot\theta\,\hat{\boldsymbol{r}}(\Omega t) + L\,\sin\theta\,\dot\theta\,\hat{\boldsymbol{z}}\end{aligned}$$

Kinetic energy and potential energy are

$$T = \frac{m}{2}\,\dot{\boldsymbol{x}}^2 = \frac{m}{2}\left[L^2\,\dot\theta^2 + (R + L\,\sin\theta)^2\,\Omega^2\right]$$

$$V = -mgL\,\cos\theta$$

and the Euler-Lagrange equation for $\theta(t)$ take the form

$$m\,L^2\,\ddot\theta(t) = \frac{d}{dt}\frac{\partial\mathcal{L}}{\partial\dot\theta} = \frac{\partial\mathcal{L}}{\partial\theta} = m\,\Omega^2\,(R + L\,\sin\theta)\,\cos\theta - mgL\,\sin\theta$$

We introduce

- the eigenfrequency of the hanging arm, $\omega = \sqrt{g/L}$
- the ratio of frequencies, $\tau = \Omega/\omega$
- the ratio of the length of the arms, $\lambda = R/L$

and absorb ω into the dimensionless time scale. Thus, we find

$$\ddot\theta = \tau^2\,(\lambda + \sin\theta)\,\cos\theta - \sin\theta$$

which admits a conserved energy-like quantity

$$\mathcal{E} = \frac{\dot\theta^2}{2} + U_{\text{eff}}(\theta)$$

with an effective potential

$$U_{\text{eff}}(\theta) = -\frac{\tau^2}{2}\,(\lambda + \sin\theta)^2 - \cos\theta$$

The left panel of Figure 6.12 shows the effective potential for a fixed ratio $L/R = 4$ and different values of Ω/ω. For small frequencies, $\Omega/\omega = 0.2$, the masses are pushed outwards such that the

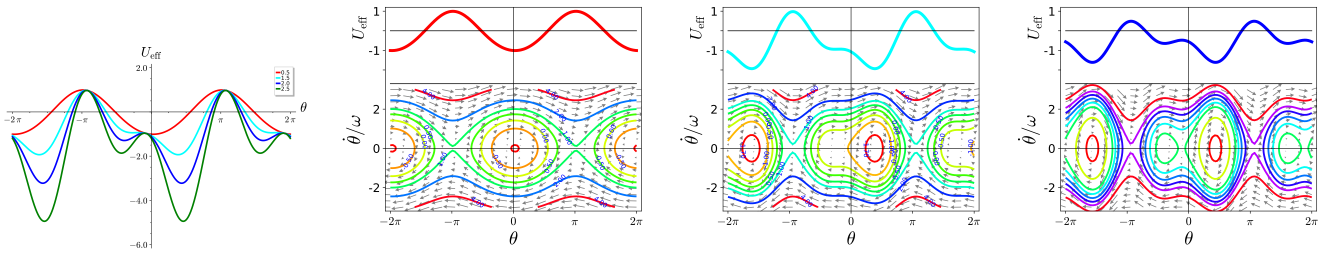

Figure 6.12: The effective potential (left) and phase space plots for the parameter values $L = 4R$ and $\Omega/\omega = 0.5$, 1.5 and 2.0 (from left to right).

equilibrium position is no longer at $\theta = 0$. Otherwise, the phase space plot looks like the one of a mathematical pendulum. For increasing $\tau = \Omega/\omega$ a shoulder emerges in the potential, and for $\tau > \tau_c \simeq 1.5$ this leads to the emergence of a new minimum with $-\pi/2 < \theta_- < 0$. It is separated from the previous minimum by a maximum at θ_+ with $-\theta_- \gg -\theta_+ > 0$. For $\tau > \tau_c$ there are two stable fixed points that lie in regions surrounded by homoclinic trajectories that start and end at θ_+. Further outside there are oscillating trajectories that move around both fixed points, and beyond the heteroclinic trajectories that connect the maxima of the potential one finds trajectories that keep rotating in the same direction.

When increasing the rotation frequency beyond τ_c a second stable solution emerges in the system by a saddle-node bifurcation. To find the parameters where it emerges we observe that fixed points emerge at positions θ where the effective force vanishes

$$\sin\theta = \tau^2\ (\lambda + \sin\theta)\ \cos\theta$$

$$\Rightarrow \quad \lambda_\tau(\theta) = \frac{\tan\theta}{\tau^2} - \sin\theta$$

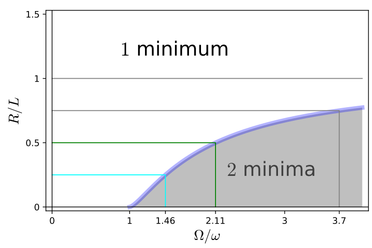

Figure 6.13: Phase diagram with positions of the bifurcations as function of τ and λ.

for $\tau < 1$ the function $\lambda_\tau(\theta)$ is monotonous. Hence, there is a single fixed point.

for $\tau < 1$ the function $\lambda_\tau(\theta)$ has a maximum and a minimum. For values of λ between these extrema there are three solution.

The extrema of $\lambda_\tau(\theta)$ lie at

$$0 = \frac{d\lambda}{d\theta} = \frac{1}{\tau^2}\,\frac{1}{\cos^2\theta} - \cos\theta \qquad \Rightarrow \qquad \cos\theta = \tau^{-2/3}$$

The maximum of λ therefore takes the value

$$\lambda_c = \sin\theta\,\left(\frac{1}{\tau^2\,\cos\theta} - 1\right) = -\sqrt{1-\cos^2\theta}\,\left(\frac{1}{\tau^2\,\cos\theta} - 1\right) = \left(1 - \tau^{-4/3}\right)^{3/2}$$

eigenvalues of linearized EOM, normal forms of bifurcations

6.3.5 *Self Test*

Problem 6.1. **Phase-space analysis for a pearl on a rotating ring**

a) Verify then by explicit calculation that $\hat{\boldsymbol{R}}$, $\hat{\boldsymbol{\theta}}$, and $\hat{\boldsymbol{\phi}}$ obey the relations

$$\hat{\boldsymbol{\theta}} = \frac{\partial \hat{\boldsymbol{R}}}{\partial \theta} \qquad \text{and} \qquad \hat{\boldsymbol{\phi}} = \hat{\boldsymbol{R}} \times \hat{\boldsymbol{\theta}} \, ,$$

and that they form an orthonormal basis.
How is $\hat{\boldsymbol{\phi}}$ related to $\partial \hat{\boldsymbol{R}} / \partial \phi$?

b) Evaluate $\dot{\boldsymbol{x}}(t) = \ell \, \dot{\hat{\boldsymbol{R}}}(\theta(t), \Omega t)$ based on the relations established in a).

c) Determine the kinetic energy T and the potential energy V of the pearl.

d) Fill in the steps in the derivation of the EOM for θ, as provided in Equation (6.3.3).

Problem 6.2. **Kitchen pendulum**

We consider a pendulum that is built from two straws (length L_1 and L_2), two corks (masses m_1 and m_2), a paper clip, and some Scotch tape (see picture to the right). It is suspended from a shashlik skewer, and its motion is stabilized by means of the spring taken from a discharged ball-pen. Hence, the arms move vertically to the skewer. We denote the angle between the arms as α, and the angle of the right arm with respect to the horizontal as $\theta(t)$.

Figure 6.14: Setup of the kitchen pendulum.

a) Determine the kinetic energy, T, and the potential energy, V, of the pendulum. Argue that T and V can only depend on θ and $\dot{\theta}$, and determine the resulting Lagrangian $\mathcal{L}(\theta, \dot{\theta})$.

b) Determine the EOM of the pendulum.

c) Find the rest positions of the pendulum, and discuss the motion for small deviations from the rest positions. Sketch the according motion in phase space.

d) The EOM becomes considerably more transparent when one selects the center of mass of the corks as reference point. Show that the center of mass lies directly below the fulcrum when the pendulum it at rest.

e) Let ℓ be the distance of the center of mass from the fulcrum, and $\varphi(t)$ be the deflection of their connecting line from the vertical. Determine the Lagrangian $\mathcal{L}(\varphi, \dot{\varphi})$ and the resulting EOM for $\varphi(t)$.

f) Do you see how the equations for $\ddot{\theta}(t)$ and $\ddot{\varphi}(t)$ are related?

6.4 *Dynamics with two degrees of freedom*

6.4.1 *The EOM for the spherical pendulum*

The spherical pendulum describes the motion of a mass M that is mounted on a bar of fixed length ℓ whose other end is fixed to a pivot. Thus, the position of the mass is constraint to a spherical shell. We adopt spherical coordinates to describe the position

$$\boldsymbol{x}(t) = \ell \begin{pmatrix} \sin\theta(t)\ \cos\phi(t) \\ \sin\theta(t)\ \sin\phi(t) \\ -\cos\theta(t) \end{pmatrix} = \ell\, \hat{\boldsymbol{R}}\big(\theta(t), \phi(t)\big)$$

The angle θ takes values $0 < \theta < \pi$, and it denotes the angle between the position the mass and the gravitational field. Consequently, the potential energy in the gravitational field is obtained

$$U = -M\,\boldsymbol{g}\cdot\boldsymbol{x} = -M\,g\,\ell\,\cos\theta(t)\,.$$

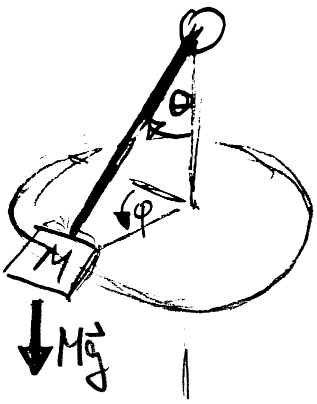

Figure 6.15: Spherical coordinates adopted to describe the motion of a spherical pendulum.

The angle ϕ takes values $0 \le \phi < 2\pi$, and it describes in which direction the mass is deflected from the vertical line, in a plane orthogonal to the action of gravity (see Figure 6.15).

For the velocity we find

$$\begin{aligned}\dot{\boldsymbol{x}} &= \ell\,\dot\theta\,\partial_\theta \hat{\boldsymbol{R}}\big(\theta(t),\phi(t)\big) + \ell\,\dot\phi\,\partial_\phi \hat{\boldsymbol{R}}\big(\theta(t),\phi(t)\big) \\ &= \ell\,\dot\theta\,\hat{\boldsymbol{\theta}}\big(\theta(t),\phi(t)\big) + \ell\,\dot\phi\,\sin\theta(t)\ \hat{\boldsymbol{\phi}}\big(\theta(t),\phi(t)\big)\end{aligned}$$

where we introduced $\hat{\boldsymbol{\theta}}$, and $\hat{\boldsymbol{\phi}}$ with

$$\hat{\boldsymbol{\theta}}(\theta,\phi) = \begin{pmatrix} \cos\theta\ \cos\phi \\ \cos\theta\ \sin\phi \\ \sin\theta \end{pmatrix} \quad\text{and}\quad \hat{\boldsymbol{\phi}}(\theta,\phi) = \begin{pmatrix} -\sin\theta\ \sin\phi \\ \sin\theta\ \cos\phi \\ 0 \end{pmatrix}$$

The unit vectors $\hat{\boldsymbol{R}}$, $\hat{\boldsymbol{\theta}}$, and $\hat{\boldsymbol{\phi}}$ form a position-dependent orthonormal basis that describes positions in $\mathbb{R}^3$ in terms of polar coordinates. The expression for $\dot{\boldsymbol{x}}$ and $\hat{\boldsymbol{\theta}}\cdot\hat{\boldsymbol{\phi}} = 0$ immediately provide the kinetic energy

$$T = \frac{M}{2}\,\dot{\boldsymbol{x}}^2 = \frac{M}{2}\,\ell^2\,\dot\theta^2(t) + \frac{M}{2}\,\ell^2\,\sin^2\theta(t)\,\dot\phi^2(t)$$

Consequently, the Lagrange function for the spherical pendulum takes the form

$$\mathcal{L}(\theta,\phi,\dot\theta,\dot\phi) = \frac{M}{2}\,\ell^2\,\dot\theta^2 + \frac{M}{2}\,\ell^2\,\sin^2\theta(t)\,\dot\phi^2(t) + M\,g\,\ell\,\cos\theta(t)$$

We observe that $\mathcal{L}$ does not depend on ϕ. In that case it is advisable to first discuss the EOM for ϕ. It takes the form

$$M\,\ell^2\,\frac{\mathrm{d}}{\mathrm{d}t}\Big(\dot\phi\,\sin^2\theta(t)\Big) = \frac{\mathrm{d}}{\mathrm{d}t}\frac{\partial\mathcal{L}}{\partial\dot\phi} = \frac{\partial\mathcal{L}}{\partial\phi} = 0$$

The derivative of the Lagrange function with respect to ϕ vanishes because $\mathcal{L}$ does not depend on ϕ. Such a coordinate is called a cyclic, and it always implies a conservation law, C. For the spherical pendulum it signifies conservation of the z-component of the angular momentum, and it provides an expression of $\dot\phi$ in terms of θ

$$C = \dot\phi\,\sin^2\theta(t) = \text{const} \quad\Rightarrow\quad \dot\phi(t) = \frac{C}{\sin^2\theta(t)} \tag{6.4.1}$$

where C is proportional to the z-component of the angular momentum.

The general case is summarized in the following definition:

Definition 6.7: Cyclic coordinates

A coordinate q_i is called *cyclic* when the Lagrange function depends only on its time derivative $\dot{q}_i$, and not on q_i. In that case the associated Euler-Lagrange equation establishes a conservation law,

$$C = \frac{\partial \mathcal{L}}{\partial \dot{q}_i}$$

After all
$$\frac{\mathrm{d}\, C}{\mathrm{d}t} = \frac{\mathrm{d}}{\mathrm{d}t} \frac{\partial \mathcal{L}}{\partial \dot{q}_i} = \frac{\partial \mathcal{L}}{\partial q_i} = 0$$

Remark 6.2. The constant value of C is determined by the initial conditions on $\dot{q}_i$ and on the other coordinates.

Let us now consider to the other coordinate of the spherical pendulum. The EOM for $\theta(t)$ takes the form

$$\begin{aligned} M\,\ell^2\,\ddot{\theta}(t) &= \frac{\mathrm{d}}{\mathrm{d}t} \frac{\partial \mathcal{L}}{\partial \dot{\theta}} \\ &= \frac{\partial \mathcal{L}}{\partial \theta} = M\,\ell^2\,\dot{\phi}^2(t)\;\sin\theta(t)\;\cos\theta(t) - M\,g\,\ell\,\sin\theta(t) \end{aligned}$$

In this equation the unknown function $\dot{\phi}(t)$ can be eliminated by means of the conservation law, Equation (6.4.1), yielding

$$\ddot{\theta}(t) = \frac{C^2\,\cos\theta(t)}{\sin^3\theta(t)} - \frac{g}{\ell}\,\sin\theta(t)$$

and the resulting EOM can be integrated once by multiplication with $2\dot{\theta}(t)$

$$\begin{aligned} \dot{\theta}^2(t) - \dot{\theta}^2(t_0) &= \int_{t_0}^{t} \mathrm{d}t\, 2\dot{\theta} \left(\frac{C^2\,\cos\theta(t)}{\sin^3\theta(t)} - \frac{g}{\ell}\,\sin\theta(t) \right) \\ &= -2 \int_{\theta(t_0)}^{\theta(t)} \mathrm{d}\theta\, \frac{\mathrm{d}}{\mathrm{d}\theta} \left(-\frac{C^2}{\sin^2\theta} + \frac{g}{\ell}\,\cos\theta \right) \end{aligned}$$

The result can be written in the form

$$E = \frac{\dot{\theta}^2}{2} + \Phi_{\text{eff}}(\theta) = \text{const}$$
$$\text{where} \quad \Phi_{\text{eff}}(\theta) = \frac{C^2}{\sin^2\theta} - \frac{g}{\ell}\,\cos\theta$$

Again a closed solution for $\theta(t)$ is out of reach. However, $\Phi_{\text{eff}}(\theta)$ can serve as an effective potential for the 1DOF motion of θ with kinetic energy $\dot{\theta}^2/2$. This interpretation of the dynamics provides ready access to a qualitative discussion of of the solutions of the EOM based on a phase-space plot.

For $C = 0$ the particle swings in a fixed plane selected by $\phi =$ const. Its motion amounts to that of a mathematical pendulum.

Figure 6.16 shows the effective potential and phase space portraits for different positive values of C. Conservation of angular momentum implies that for $C \neq 0$ the particle can no longer access the region close to its rest position at the lowermost point of the

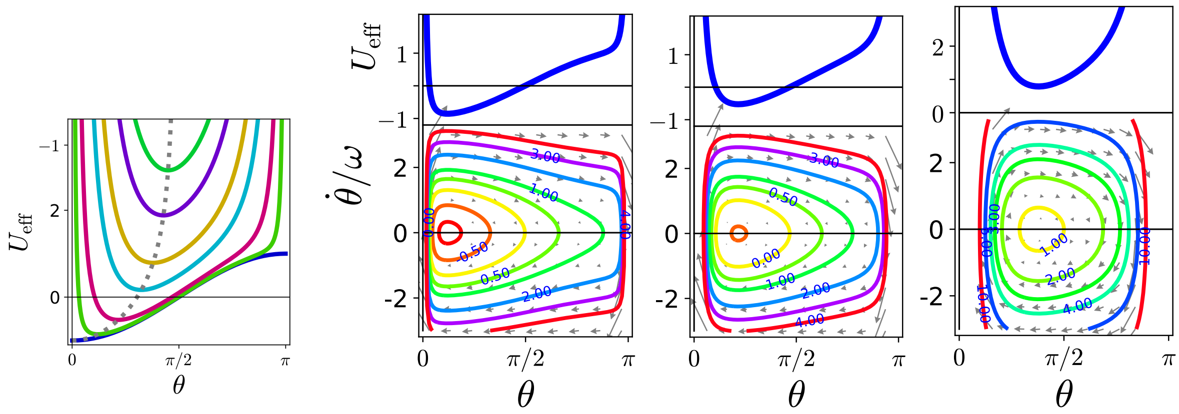

Figure 6.16: The left panel shows the effective potential for the spherical pendulum at parameter values $C^2 \in \{0, 0.01, 0.1, 0.5, 1, 2, 3\}$ from bottom to top. The subsequent panels show phase-space portraits of the motion for $C^2 = 0.01$, 0.1, and 1, respectively.

add problem: rotation barrier

sphere. Rather it always has to go in circles around the bottom of the well, and the sign of C specifies whether it moves clockwise or anti-clockwise. The divergence of the effective potential at $\theta = \pm\pi$ is called *rotation barrier*. It emerges due to a combination of the conservation of energy and angular momentum.

The effective potential has a single minimum for $0 < \theta_c(C) < \pi/2$, and not further extrema. The minimum describes motion where the particle moves at constant height with a constant speed in a circle. When this orbit is perturbed oscillations are superimposed on the circular motion. In a projection to the plane vertical to the action of gravity, this will lead to trajectories similar to those drawn by a Spirograph, Problem 2.42.

The take-home message of this example is that cyclic variables entail conservation laws of the dynamics. In the very same manner as for the Kepler problem they can be used to eliminate a variable from the EOM of the other coordinates. The additional contributions in the EOMs for the other coordinate(s) are interpreted as part of an effective potential.

6.4.2 *Double pendulum*

6.5 *Dynamics of 2-particle systems*

revisit Kepler

6.6 *Conservation laws, symmetries, and the Lagrange formalism*

6.7 *Worked problems: spinning top and running wheel*

spinning top

rolling wheel

6.8 Problems

horizontal driven double pendulum

stabilizing satellites

Lagrange points

steel can pendulum

Bibliography

Archimedes, 1878, in *Pappi Alexandrini Collectionis, Book VIII, c. AD 340*, edited by F. O. Hultsch (Apud Weidmannos, Berlin), p. 1060, cited following https://commons.wikimedia.org/wiki/File:Archimedes_lever,_vector_format.svg.

Arnol'd, V. I., 1992, *Ordinary Differential Equations* (Springer, Berlin).

Epstein, L. C., 2009, *Thinking Physics, Understandable Practical Reality* (Insight Press, San Francisco).

Finney, G. A., 2000, American Journal of Physics **68**, 223–227.

Gale, D. S., 1970, American Journal of Physics **38**, 1475.

Gommes, C. J., 2010, Am. J. Phys. **78**, 236.

Großmann, S., 2012, *Mathematischer Einführungskurs für die Physik* (Springer), very clear introduction of the mathematical concepts for physics students., URL https://doi.org/10.1007/978-3-8348-8347-6.

Harte, J., 1988, *Consider a spherical cow. A course in environmental problem solving* (University Science Books, Sausalito, CA).

Kagan, D., L. Buchholtz, and L. Klein, 1995, Phys.Teach. **33**, 150.

Lueger, O., 1926–1931, *Luegers Lexikon der gesamten Technik und ihrer Hilfswissenschaften* (Dt. Verl.-Anst., Stuttgart), URL https://digitalesammlungen.uni-weimar.de/viewer/resolver?urn=urn:nbn:de:gbv:wim2-g-3163268.

Mahajan, S., 2010, *Street-fighting Mathematics. The Art of Educated Guessing and Opportunistic Problem Solving* (MIT Press, Cambridge, MA), ISBN 9780262514293 152, some parts are available from the author, URL https://mitpress.mit.edu/books/street-fighting-mathematics.

Morin, D., 2007, *Introduction to Classical Mechanics* (Cambridge), comprehensive introduction with a lot of exercises—many of them with worked solutions. The present lectures cover the Chapters 1–8 of the book. I warmly recomment to study Chapters 1 and 6., URL https://scholar.harvard.edu/david-morin/classical-mechanics.

Morin, D., 2014, *Problems and Solutions in Introductory Mechanics* (CreateSpace), a more elementary introduction with a lot of solved exercises self-published at Amazon. Some Chapters can also be downloaded from the autor's home page, URL `https://scholar.harvard.edu/david-morin/mechanics-problem-book`.

Murray, J., 2002, *Mathematical Biology* (Springer).

Nordling, C., and J. Österman, 2006, *Physics Handbook for Science and Engineering* (Studentlitteratur, Lund), 8 edition, ISBN 91-44-04453-4, quoted after Wikipedia's List of humorous units of measurement, accessed on 5 May 2020.

Purcell, E. M., 1977, American Journal of Physics **45**(3).

Seifert, H. S., M. W. Mills, and M. Summerfield, 1947, American Journal of Physics **15**(3), 255.

Sommerfeld, A., 1994, *Mechanik*, volume 1 of *Vorlesungen über theoretische Physik* (Harri Deutsch, Thun, Frankfurt/M.).

Zee, A., 2020, *Fly by Night Physics: How Physicists Use the Backs of Envelopes* (Princeton UP), ISBN 9780691182544.